Author comment to anonymous Referee 1

Thanks for this work, try to develop a robust algorithm to generate global offshore oil and gas datasets from satellite observations. The methodology and results look reliable and reasonable. I have several comments for your reference.

We sincerely thank you for the positive assessment of our work and constructive comments, which have helped us substantially improve the manuscript. The reviewer's comments have prompted us to substantially improve the manuscript in several key aspects, including clarifying the detection pipeline and adding a comprehensive parameter sensitivity and uncertainty analysis. We have carefully addressed each comment point-by-point below, and we hope that the revised manuscript meets the expectations of the reviewer and the journal.

1. Fig. 3, why do you only use Sentinel-2 satellite imagers during Jan-Mar for OOGP generation?

Thank you for pointing this out. We apologize for any confusion caused by this. The original Fig. 3 in the manuscript contained a display issue in the x-axis labeling, which incorrectly suggested that only January-March Sentinel-2 images were used. In reality, Sentinel-2 imagery covering the full study period (2017-2023) was used, consistent with the description in Section 2.2. The figure has been corrected in the revised manuscript to accurately reflect the complete temporal coverage of the Sentinel-1 and Sentinel-2 datasets.

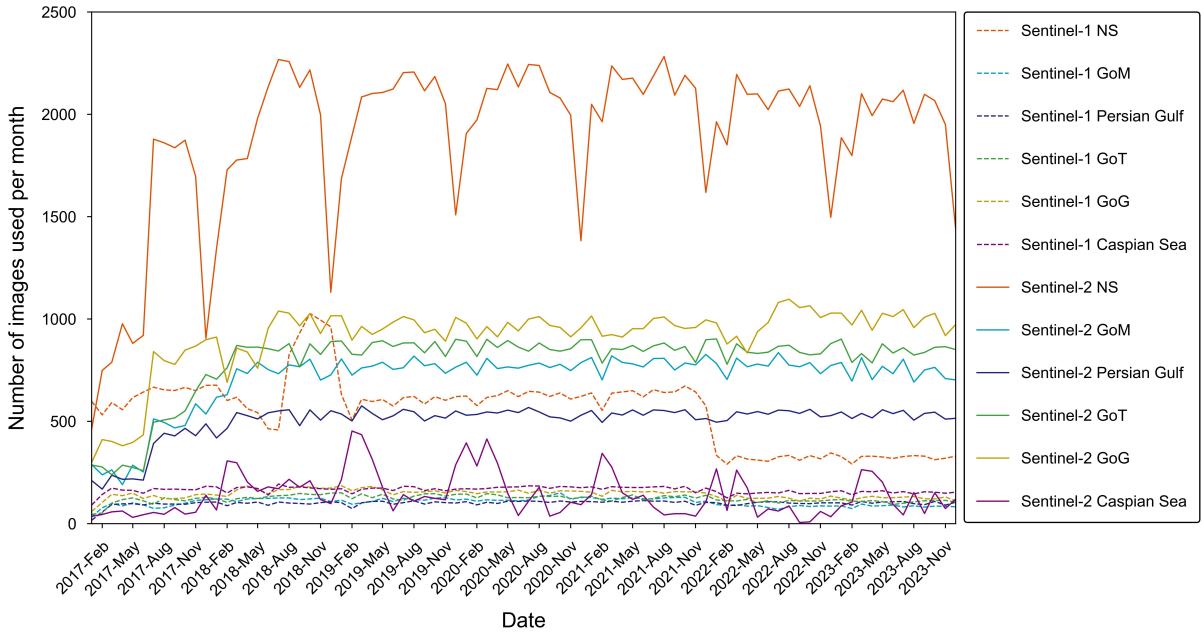

Figure 1: Statistics of the number of Sentinel-1 and Sentinel-2 images used in this study.

2. L155-160, the FIRMS with 1-km spatial resolution, Near-real time frequency was used to identify platform activity status. This is an interesting point and skillful solution. The key challenge is how to address the discrepancy in spatiotemporal resolutions between

this fire data and Sentinel-1/2 data (with 10-60 m resolution). Please add more details on this point. For example, how is proximity defined in the proposed approach?

We clarify that FIRMS data were used exclusively for spatial validation of platform activity status, not for attribute generation. The spatial resolution discrepancy between FIRMS and the primary datasets was addressed through a vector-based spatial overlay. Annual FIRMS hotspot point clouds were aggregated into cluster polygons representing areas of persistent thermal activity, and OOGPs whose centroids fell within these polygons were considered spatially validated. This polygon-based approach does not require pixel-level resolution matching. All detections were further confirmed through multi-source visual interpretation using Sentinel-2 MSI imagery, Google Earth high-resolution images, and authoritative databases (NOAA, BSEE, OGIM, and OESNS), as detailed in Section 4.1.1. To address this point, we have revised the relevant sentences in Section 2.3.2 to explicitly describe the spatial aggregation approach and clarify how the resolution discrepancy was handled. The revised text is as follows:

> L167-L173: Annual FIRMS hotspot point clouds were spatially aggregated into cluster polygons representing areas of persistent thermal activity, and OOGPs whose centroids fell within these polygons were considered spatially validated as active platforms. This vector-based spatial overlay approach is inherently robust to the resolution discrepancy between FIRMS and the primary satellite datasets, as it operates on vector geometries rather than requiring pixel-level resolution matching. By overlaying these thermal cluster polygons and dense ship lane polygons onto satellite-detected platform locations, the auxiliary datasets ensure the accuracy of platform identification and distinguish operational platforms from other structures or false positives. All detections were further confirmed through multi-source visual interpretation as described in Section 4.1.1.

3. L160, as mentioned above, FIRMS has a different spatiotemporal resolution from the primary satellite data (Sentinel-1/2). Please clarify this point.

Annual FIRMS hotspot point clouds were aggregated into cluster polygons representing areas of persistent thermal activity, and OOGPs whose centroids fell within these polygons were considered spatially validated. This approach is inherently robust to resolution differences, as it operates on vector geometries rather than raster pixels. A clarifying sentence has been added to Section 2.3.2 of the revised manuscript. The revised text in Section 2.3.2 is provided above.

4. Eq.(1), although two local examples are given to demonstrate the rationale regarding the BCmax threshold of -20db, an adaptive threshold like Eq. (2) is more reliable.

We thank the reviewer for this constructive suggestion. We agree that presenting a fixed absolute BC_{max} threshold (original Eq. 1) alongside the adaptive percentile threshold (Eq. 2) created unnecessary ambiguity regarding the actual detection workflow. We wish to clarify that

the fixed threshold was considered during early method development but was ultimately not adopted in the final detection pipeline of this study. To avoid confusion, the corresponding text and Eq. 1 have been removed from Section 3.1 of the revised manuscript. The adaptive percentile threshold, formerly Eq. 2, has been renumbered as Eq. 1 in the revised manuscript.

To provide the quantitative justification requested by the reviewer, we conducted a sensitivity analysis of five absolute BC_{max} thresholds (-15, -18, -20, -22, and -25 dB) across 12 representative OOGP locations in the GoM (Fig. 2 of this response document, corresponding to Fig. S2 of the revised manuscript). Two key findings were obtained.

First, platform targets consistently produce BC_{max} values well above all tested thresholds, confirming robust detectability regardless of the exact cutoff value.

Second, the proportion of sea surface background pixels falling below any given fixed threshold varies substantially across regions and seasons, demonstrating that a fixed absolute cutoff lacks the regional adaptability required for consistent OOGP detection.

These findings collectively justify the exclusive use of the adaptive percentile threshold as the initial detection criterion in the revised manuscript. The revised text in Section 3.1 is as follows:

> L185-L195: The backscattering coefficients in the VH band of Sentinel-1 effectively distinguish OOGPs from open water. As demonstrated by a sensitivity analysis of absolute BC_{max} thresholds across 12 representative OOGP locations in the GoM (Fig. S2), fixed absolute cutoffs lack regional adaptability due to substantial variability in sea-surface background backscatter across regions and seasons. Therefore, the detection framework adopts the percentile-based adaptive threshold described in Section 3.2, which dynamically adjusts to the local backscatter distribution of each region and month. The detection framework is based on the physical differences between fixed OOGPs and mobile objects, such as vessels: OOGPs produce stable and temporally persistent backscatter signals, whereas vessels generate decorrelated and spatially variable signals with low OF values. Exploiting these differences, platform detection proceeds in two complementary stages. In the first stage, a percentile-based adaptive threshold was applied to identify candidate targets with high completeness. In the second stage, the OF filtering removed the transient signals. Together, the percentile threshold governs candidate set completeness, while the OF filter governs false positive suppression. The theoretical justification and sensitivity analyses for each stage are detailed in Sections 3.2 and 3.3.1 respectively.

5. Fig. 10, how can we control the effect of the uncertainty in satellite data and algorithm (like threshold selection) on these temporal variations?

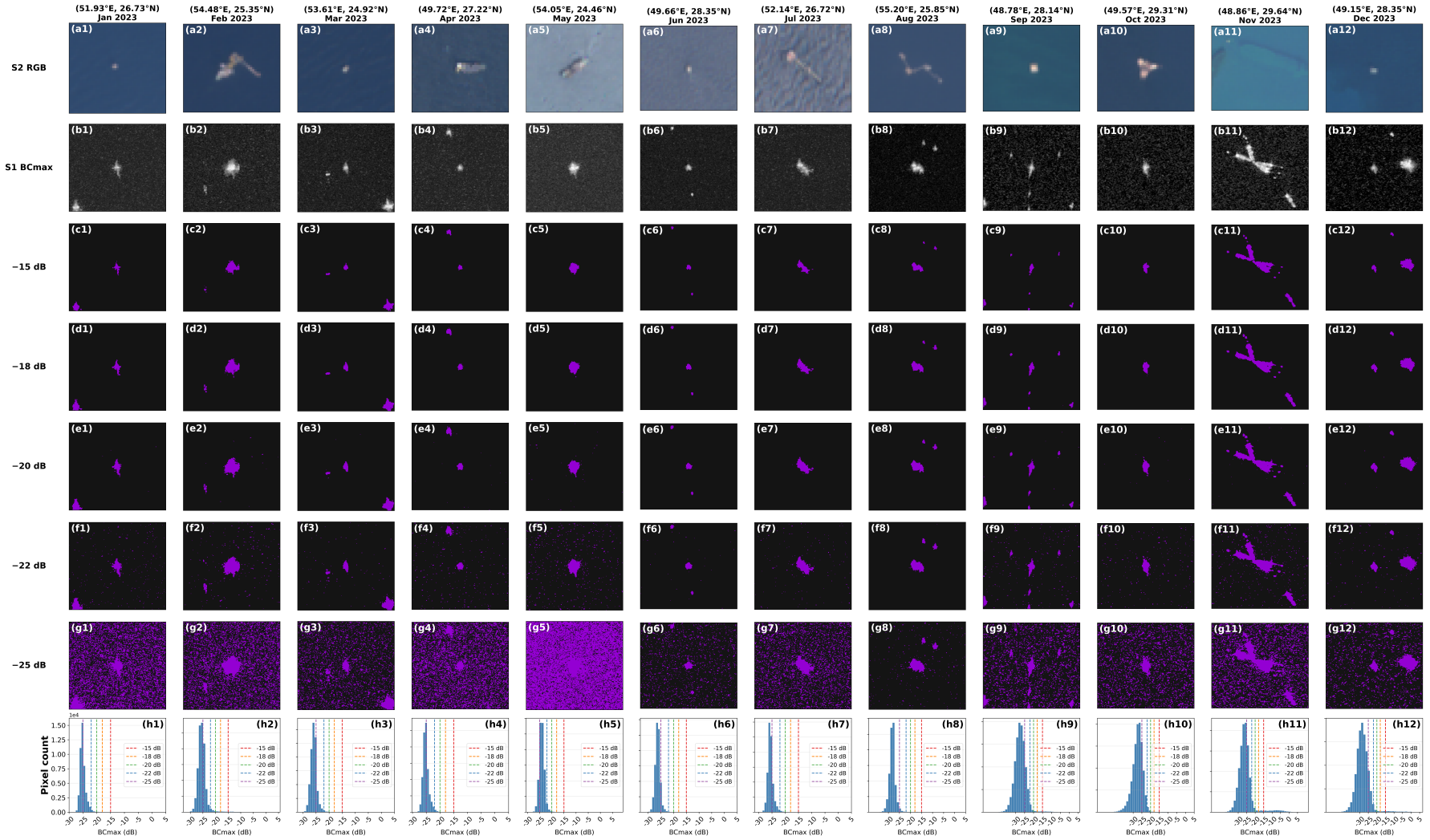

Figure 2: Sensitivity of absolute BC_{max} thresholds at 12 representative OOGP locations in the GoM (2023). Each column corresponds to one platform location, labelled by coordinates and acquisition month. Rows show: (a1-a12) Sentinel-2 true-color imagery using a 200 m buffer; (b1-b12) Sentinel-1 monthly BC_{max} in VH polarization using a 1000 m buffer, shown in grayscale; (c1-c12) to (g1-g12) binary retention masks under absolute thresholds of −15, −18, −20, −22, and −25 dB, respectively; and (h1-h12) histograms of BC_{max} pixel values within the 1000 m buffer, with the five candidate thresholds indicated by vertical dashed lines. Purple pixels indicate values exceeding the threshold and are therefore retained, whereas black pixels indicate values below the threshold and are therefore excluded.

As shown in Fig. 10 in the revised manuscript and Fig. 3 in this response letter, we conducted a parameter sensitivity analysis of the region-specific OF thresholds and propagated the results as error bars.

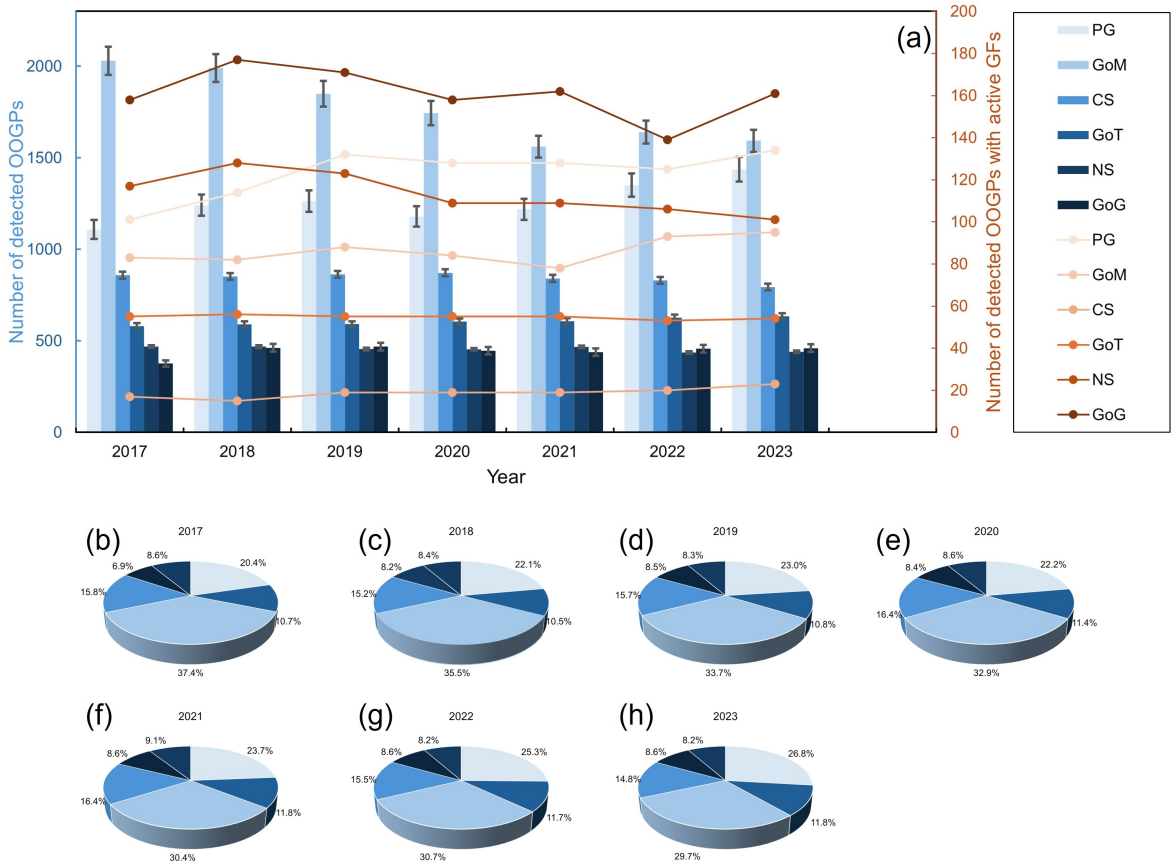

Figure 3: (a) Temporal evolution of detected OOGPs and OOGPs with active gas flarings (GFs) in select regions. (b)–(h) Proportion of each offshore basin based on the available data from 2017 to 2023. Error bars represent algorithmic uncertainty estimated from OF threshold sensitivity analysis (σ_{OF} = 1.6-4.7%; see Supplementary Material, Table S3.)

We varied each basin's OF threshold within ± 2 steps of the adopted value and computed the relative standard deviation of TP counts as the sensitivity index, σ_{OF}. The results are summarized in Table 1 (Table S3 in the Supplementary Material).

Table 1: OF threshold sensitivity analysis results by basin.

Basin	**Adopted OF**	**Test range**	σ_{OF}
GoM	3	2 - 5	3.8%
CS	3	2 - 5	2.2%
GoT	2	2 - 4	2.7%
NS	6	4 - 7	1.6%
GoG	2	2 - 4	4.6%
PG	3	2 - 5	4.7%

Error bars are calculated as

$$\delta N_{\text{year}} = N_{\text{year}} \times \sigma_{\text{OF}}$$

The PG increase of 329 platforms far exceeds its ±68 platform uncertainty and is further corroborated by independent evidence. As shown in Fig. 4 and Fig. 5 (Fig. S10 in the Supplementary Material), new detections are geographically concentrated in the Safaniya, Zuluf, and Marjan fields (Saudi Arabia), the North Dome/South Pars fields (Qatar), and the Upper Zakum fields (UAE), consistent with documented active development (Kaiser, 2022) and reports from the U.S. Energy Information Administration (`https://www.eia.gov/`). In addition, the Middle East accounted for the largest share of global unfinished offshore gas reserves in 2022 (Chen et al., 2024). These results confirm that the temporal trends in Section 4.2 reflect genuine infrastructure changes rather than algorithmic sensitivity.

The sensitivity analysis was based on 2023 validation data applied uniformly across 2017-2023, assuming the temporal stability of σ_{OF}. The results are based on validation samples rather than the full platform population and should therefore be interpreted as approximate estimates. The revised Fig. 10 includes error bars for all basins, and the methodology has been added to the supplementary file.

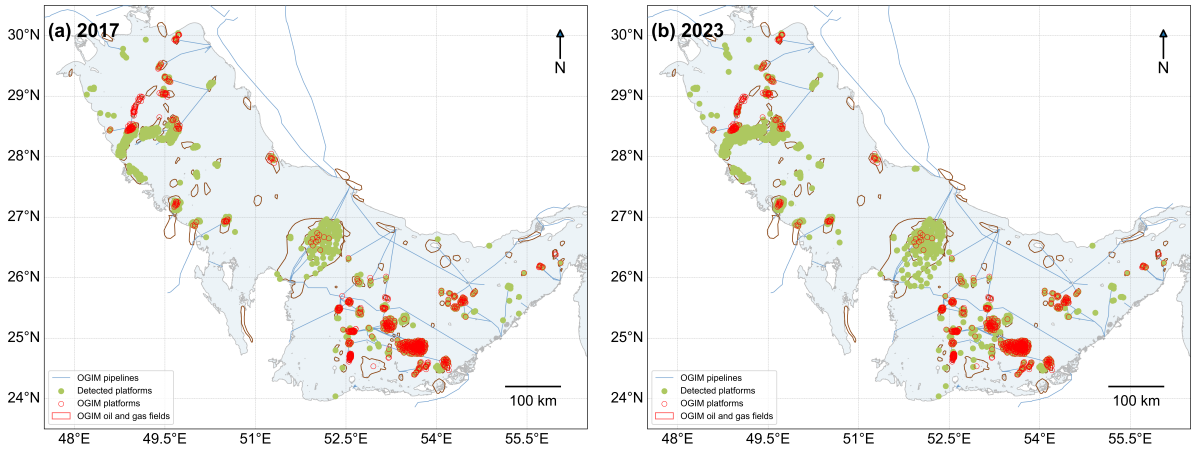

Figure 4: Spatial distribution of detected offshore oil and gas platforms and fields in the Persian Gulf between 2017 and 2023.

L382-L384: The robustness of these trends against algorithmic parameter uncertainty was assessed through an OF threshold sensitivity analysis, the methodology and results of which are provided in the Supplementary Material (Table S3).

Supplementary file: To quantify the sensitivity of the detected platform counts to the adopted OF thresholds, we varied each basin's threshold within 2 steps of the adopted value and computed the relative standard deviation of true positive counts as the sensitivity index σ_{OF}. The results are summarized in Table S3. The error bars in Fig. 10 were calculated as

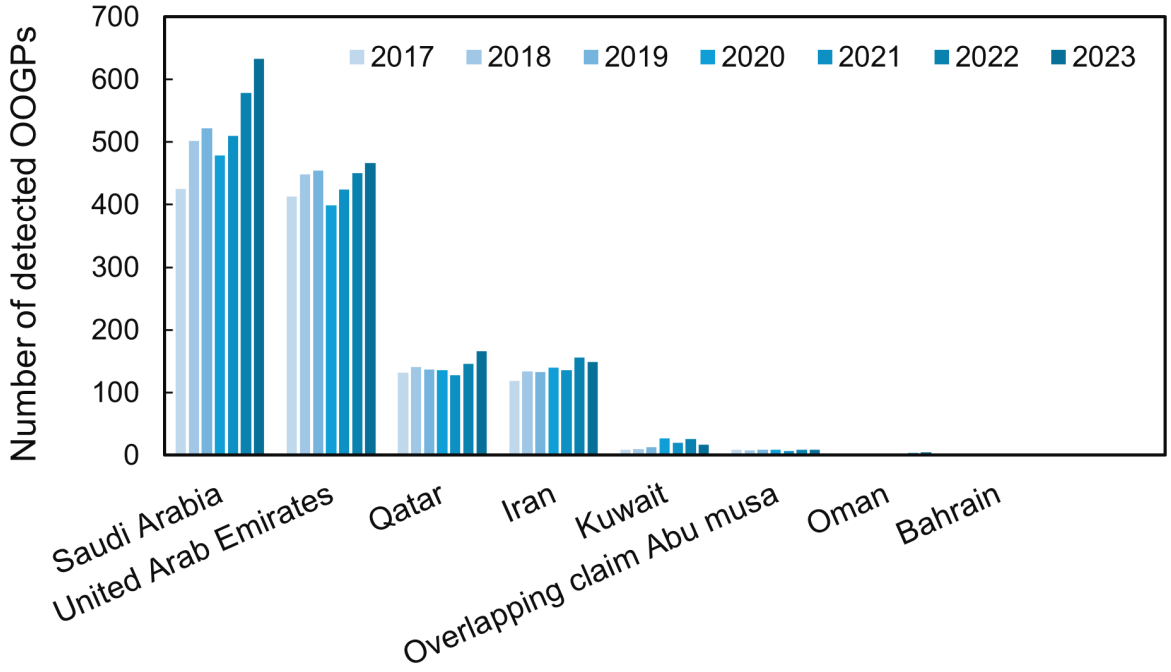

Figure 5: Temporal count changes of detected offshore oil and gas platforms between different countries in the Persian Gulf.

$\delta N_{\text{year}} = N_{\text{year}} \times \sigma_{\text{OF}}$, providing a conservative estimate of the algorithmic uncertainty in the temporal trends.

References

Chen, X., Wang, Z.-q., Li, C.-x., Gao, F., and Wei, Q.: Characteristics of Global Offshore Oil and Gas Development, https://doi.org/10.1007/978-981-97-0475-0_87, 2024.

Kaiser, M. J.: Offshore oil and gas records circa 2020, Taylor & Francis, https://www.tandfonline.com/doi/abs/10.1080/17445302.2020.1827633, publisher: Taylor & Francis, 2022.